

Investigation of the changes in hydrogen bonding accompanying the structural reorganization at 103K in Ammonium iodate

W. G. Marshall<sup>a†</sup>, R. H. Jones<sup>b,\*</sup>, K. S. Knight<sup>a,c,d</sup>, C. R. Pulham<sup>e</sup> and R. I. Smith<sup>a</sup>

a ISIS Facility, STFC Rutherford Appleton Lab, Harwell Oxford, Didcot OX11 0QX, Oxon, England Fax 44 1235 4455720 Tel 44 1235 445434

b School of Chemical and Physical Sciences, Keele University, Keele, ST5 5BG United Kingdom. Fax 44 1792 712378, Tel: 44 1782 733033,

<sup>c</sup> Department of Earth Sciences

c Department of Earth Sciences, University College London, Gower Street, London, WC1E 6BT United Kingdom

d Department of Earth Sciences, The Natural History Museum, Cromwell Road, London, SW7 5BD United Kingdom

e EaStCHEM School of Chemistry, University of Edinburgh, Joseph Black Building, David Brewster Road  
Edinburgh EH9 3FJ

† Deceased.

- Correspondence e-mail [r.h.jones@keele.ac.uk](mailto:r.h.jones@keele.ac.uk)

Neutron powder diffraction has been used to observe the changes in hydrogen bonding that occur as a function of temperature in  $\text{ND}_4\text{IO}_3$ , and thus determine the structural features that occur during the low temperature (103 K) phase transition. We show that in the deuterated material the change is not a phase change *per se* but rather a structural reorganization in which the hydrogen bonding becomes “firmly locked in” at the phase transition temperature, and stays in this configuration upon further cooling to 4.2 K. In addition, both the differences and changes in the axial thermal expansion coefficients in the region 100 – 290K can be explained by the changes involving both the hydrogen bonding and secondary I---O halogen bonds.

## Introduction

Ammonium iodate has drawn interest because of its pyroelectric, (Keve, *et al* 1971) ferroelectric (Oka, *et al* 1976), electrooptical (Bismayer & Salje 1976), and ferroelastic properties (Abdel-Kader *et al.*, 2008) This compound contains both halogen and hydrogen bonds, which may be implicated in these macroscopic properties. In this work neutron powder diffraction has been used to investigate the changes in halogen and hydrogen bonding that occur as a function of temperature and relate these to some of the macroscopic properties.

The ambient-temperature orthorhombic ( $Pc2_1n$ ) crystal structure of ammonium iodate was first determined over 40 years ago (Keve, *et al* 1971). It consists of pyramidal  $\text{IO}_3^-$  anions and tetrahedral  $\text{NH}_4^+$  cations – (Figure 1a). In addition to the covalent bonds within these ions there are also distinct halogen and hydrogen bonds. In the original structural study, it was not possible to locate the hydrogen atoms, but despite this it was possible to describe the hydrogen bonding within the compound on the basis of the N---O contacts. Two of the oxygen atoms of the  $\text{IO}_3^-$  group are each involved in one hydrogen bond, whilst the third oxygen atom is implicated in two hydrogen bonds, (Figure 1b). In addition to the primary covalent bonds there are also three longer I---O contacts which are much shorter (2.778–2.830 Å) than the sum of the van der Waals radii (3.61 Å) (Rowland and Taylor 1996). Each of these longer I...O halogen contacts occupy a position which is approximately *trans* to an I-O covalent bond resulting in a highly distorted octahedral environment, (Figure 1c). If the coordination of the iodine is considered to be octahedral then the structure has been described as a highly distorted perovskite (Keve, *et al* 1971), (Figure 1 d) with the iodine being the six fold coordinated atom. The occurrence of these longer I---O contacts and the *trans* geometry found in the O-I---O moieties was commented on by Alcock in his classic review on secondary interactions in inorganic compounds (Alcock 1972). In this review he listed many interactions which have subsequently been recognised as halogen bonds (Metrangolo *et al* 2005). At the time of Alcock's review it was believed that the donor atom in the halogen bond donated a pair of electrons to the  $\sigma^*$  anti bonding orbital of the acceptor molecule in line with the then current view of the bonding in charge transfer complexes (Mulliken 1952). By contrast the current view of bonding in these (halogen bonded) complexes (which is most widely accepted) focusses on the coulombic interaction between a region of negative potential situated on the donor and a region of positive potential on the halogen, the so-called  $\sigma$ -hole (Brink *et al* 1992; Politzer & Murray 2013; Clark *et al* 2007). The  $\sigma$ -hole on the halogen lies on the axis which is an extension of the bond between the halogen and the atom to which it is bonded. This model when modified to take account of polarization and dispersion effects (Poltzer & Murray 201; Politzer *et al* 2012) has become the standard description of halogen bonding in the vast majority of such complexes (Cavallo *et al* 2016). Complexes involving halogen bonds have not only been investigated

because of the basic questions of bonding in these complexes but also because of their role in fields as diverse as supramolecular chemistry (Bertani, *et al* 2010; Rissanen 2008) liquid crystals, (Nguyen *et al* 2005; Cho *et al* 2013; McAllister *et al* 2013) and biological systems (Auffinger *et al* 2004; Scholfield *et al* 2013). In biological systems there is also the possibility of the occurrence of additional (C-H...X) interactions which may be of importance in controlling the orientation of a substrate molecule at an active site (Lu *et al* 2009). We have also shown using neutron powder diffraction that such weak additional hydrogen bond interactions do occur in several simple non-biological systems (Jones *et al* 2013, Marshall *et al* 2017, Marshall *et al* 2018) and can be responsible for properties such as colossal thermal expansion (Jones *et al* 2014). In  $\text{NH}_4\text{IO}_3$  there is the possibility of competition between both N-H...O and O-I...O bonds controlling the orientation of the primary  $\text{IO}_3^-$  units with consequent effects on macroscopic properties.

As we have noted at the outset, ammonium iodate has drawn interest because of its ferroelectric pyroelectric, electrooptical and ferroelastic properties. One ferroelectric transition is well documented and occurs at 368 K at ambient pressure (Viswanathan, & Salje, 1975), for which it was shown that in the immediate pre- and post-transition region there were a series of subtle changes in the structure. In the pre-transition region, it was observed that a contraction occurred along the polar b-axis. Later work showed that this was accompanied by a simplification of the vibrational spectrum in the N-H region to give a spectrum consistent with a tetrahedral ion in the high temperature paraelectric phase (Barabash, A., *et al* 1999). In the post-transition region there is a further change to give a cubic unit cell at 393K (Viswanathan, & Salje, 1975). A second transition has also been suggested at 103 K (Salje 1974) and a recent study reporting x-ray diffraction and dielectric permittivity results appears to confirm this (Kader *et al* 2013).

Furthermore, it is well known that hydrogen bonding can play a key role in determining the ferroelectric and related properties in both inorganic and organic systems. The prototypical system in the case of inorganic compounds is potassium dihydrogen phosphate  $\text{KH}_2\text{PO}_4$  (Busch, & Scherrer, 1935), which has been extensively studied, both as a function of temperature and pressure using both x-ray (Endo *et al* 1989; Kobayashi *et al* 1995; Cai, & Katrusiak, 2013), and neutron diffraction (Umebayashi *et al* 1967; Tibballs *et al* 1982). The N-H...O systems have also been extensively studied both in inorganic  $\text{NH}_4\text{H}_2\text{PO}_4$  (Lasave *et al* 2007; Peres *et al* 1997), and organic systems (Oleniczak *et al* 2013, Zhang *et al* 2010), under ambient and non-ambient conditions.

While the structural changes that occur during the high temperature (368 K) phase transition of  $\text{ND}_4\text{IO}_3$  have been extensively studied by a wide range of experimental methods (Viswanathan, & Salje, 1975; Barabash *et al* 1999; Barabash 1999; Oka *et al* 1976; Bergman *et al* 1969), much less attention has been devoted to the low temperature (~103K transition (Salje 1974; Kader *et al* 2013), though a

wideline proton NMR studied indicated that that at around 100K there was a second moment transition (Richards & Schaefer 1961). It was our aim in this work to establish at an atomic level the nature of the low temperature phase transition, and how this is related to possible changes in both the hydrogen and halogen bonding within this compound. In order to obtain accurate positions of light atoms (deuterium and oxygen) in the presence of the heavy iodine atoms we have carried out studies using neutron diffraction on powder samples, making use of the comparable scattering lengths of iodine ( $b = 5.28$  fm), nitrogen ( $b = 9.36$  fm), oxygen ( $b = 5.803$  fm), and deuterium ( $b = 6.671$  fm).

Figure 1 structures of (a) molecular ions, (b) hydrogen bonds, (c) secondary interactions, and (d) pseudo perovskite structure in  $\text{ND}_4\text{IO}_3$  (e) Relationship of molecular ions with respect to unit cell.

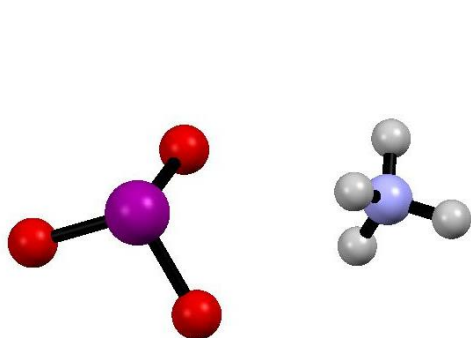


Figure 1a

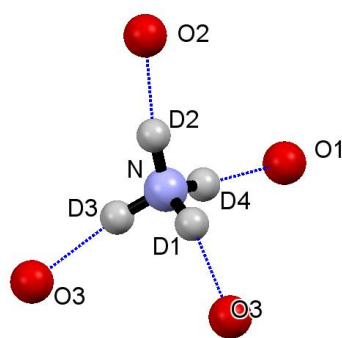


Figure1b

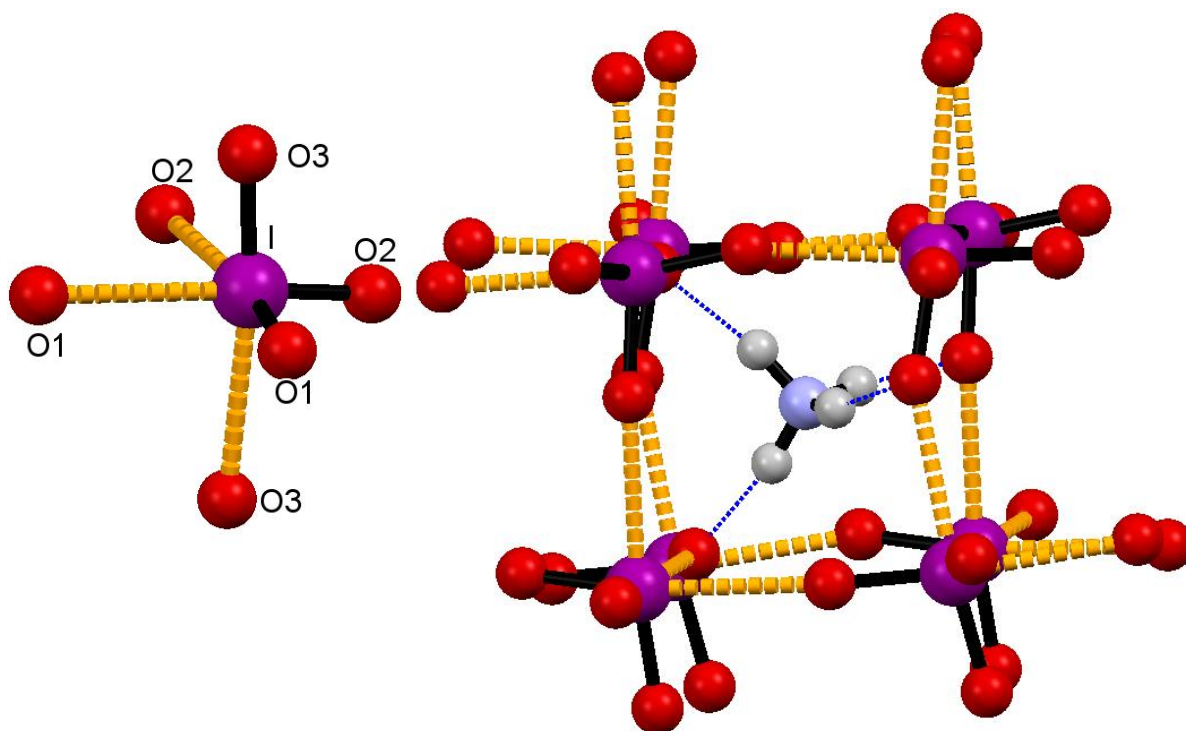


Figure1c

Figure1d

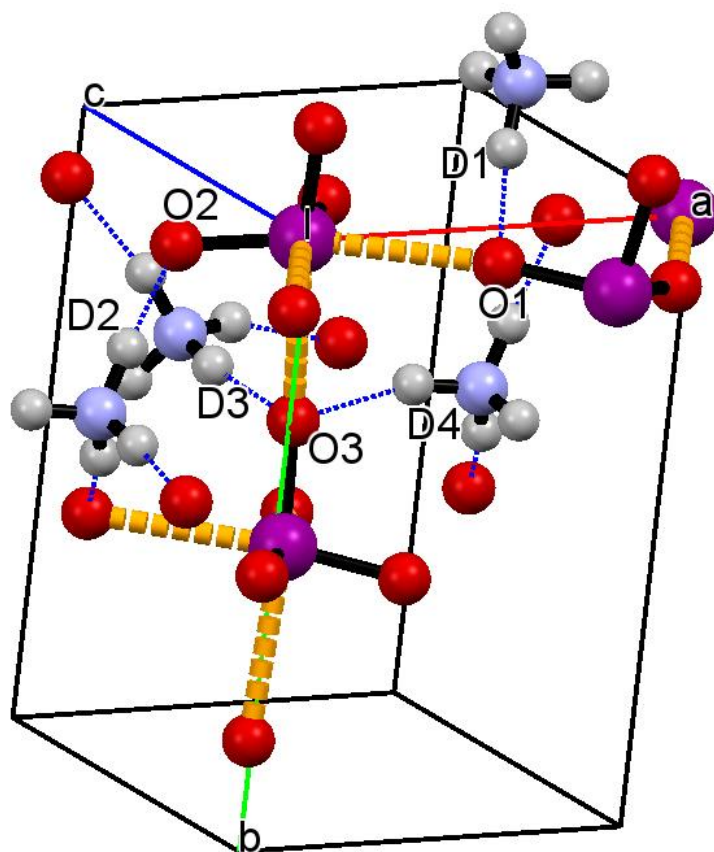


Figure1e

Hydrogen bonds are indicated by dotted blue lines, halogen bonds by dashed orange lines.'

#### Experimental

A sample of deuterated ammonium iodate was prepared by repeatedly exchanging ammonium iodate dissolved in deuterium oxide, followed by removal of solvent using a rotary evaporator attached to a diaphragm pump. Exchange was confirmed by use of infrared spectroscopy and also by the lack of any large incoherent background scattering in the neutron powder diffraction patterns which would have been observed in the presence of any significant quantity of residual hydrogenous material.

Time-of-flight neutron powder diffraction data were collected on the medium resolution powder diffractometer POLARIS at the ISIS facility Rutherford Appleton Laboratory, UK. Deuterated ammonium iodate was loaded into a 6mm diameter thin-walled vanadium sample can which was placed in a helium flow cryostat and data sets collected at 4.2K (300 $\mu$ Ah proton beam current to the ISIS target, equivalent to  $\sim$  2 hours neutron beamtime) and then from 10K to 90K in 10K steps; 95K to 120K in 5K steps; and 130K to 290K in 10K steps (all for 150 $\mu$ Ah, equivalent to  $\sim$  1 hour). Equilibration times between data sets varied from 6 minutes (5K steps) to 10 minutes (10K steps). Structure refinement was carried out by the Rietveld method (Rietveld 1969, van Laar and Schenk 2018), in Space Group  $Pc2_1n$  (consistent with the non-standard setting of space group  $Pna2_1$  used in the original study (Keve *et al* 1971)) using the GSAS (Larson & Von Dreele 2000) suite of programs through the EXPGUI graphical interface (Toby 2001). For refinement of the structure at 4.2K atomic coordinates for the non-hydrogen atoms and unit cell dimensions were taken from the literature (Keve *et al* 1971), and difference Fourier maps calculated in order to locate the deuterium atoms. For each successive higher temperature data set, starting structural and profile parameters were taken from the results of the previous lower temperature structure refinement. The final fit to the data collected at 4.2K for selected Polaris detector banks is shown in (Figure 2). The variation of unit cell parameters is shown in (Figure 3), and selected interatomic contacts and angles as a function of temperature are shown in (Figure 4), and in tabular form in full in supplementary data. A stack plot of the diffraction patterns collected over the temperature range 90 – 120K is given in (Figure 5). Thermal expansion coefficients for the linear portions of the lattice parameters were calculated using PAScal (Cliffe & Goodwin 2012), and the expansivity indicatrix is shown in (Figure 6).

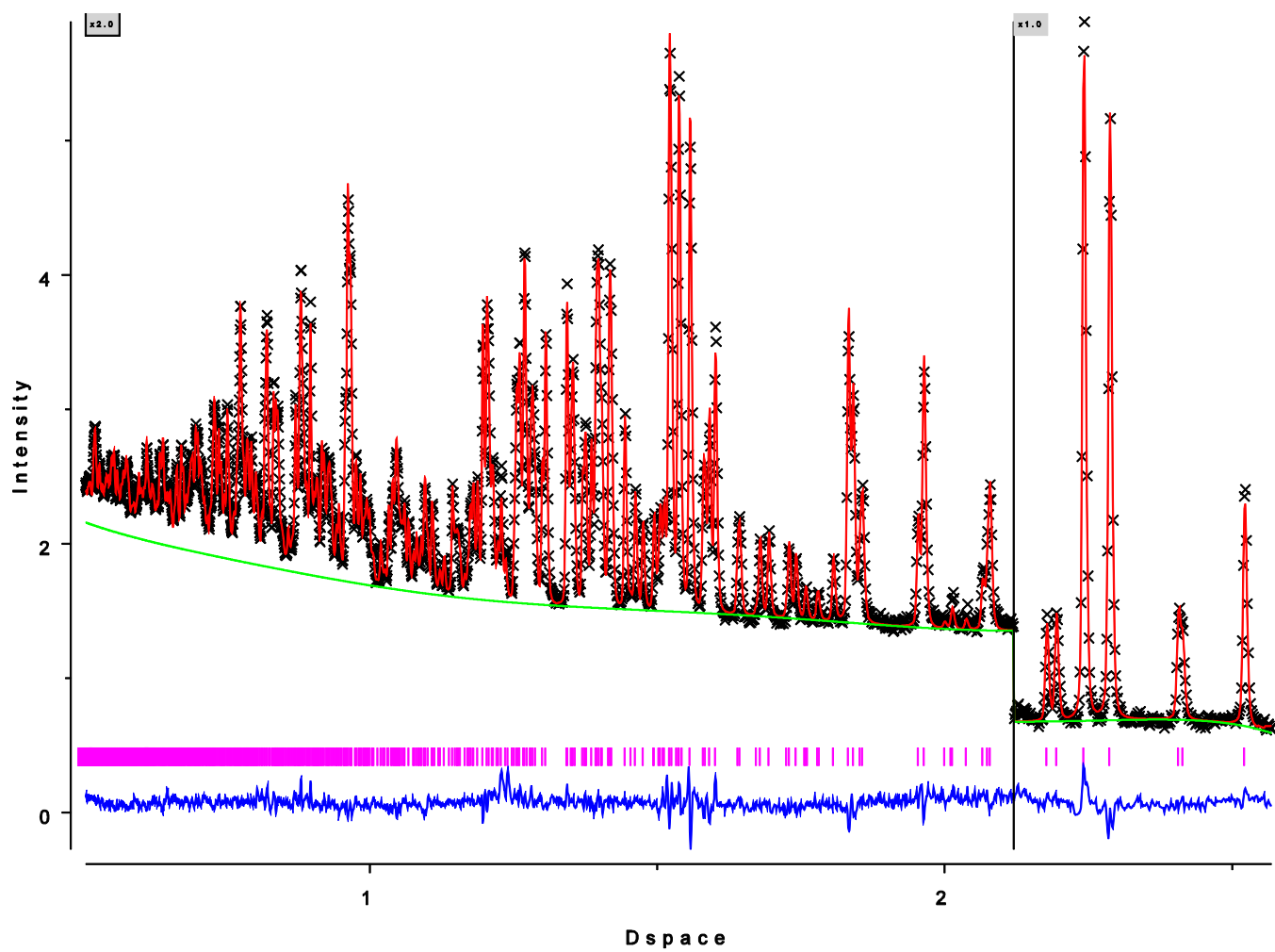


Figure 2a Fitted neutron powder diffraction data from  $\text{ND}_4\text{IO}_3$  at 4.2K collected in the Polaris backscattering detector bank ( $\langle 2\theta \rangle = 147^\circ$ ) (magnified region x 2)

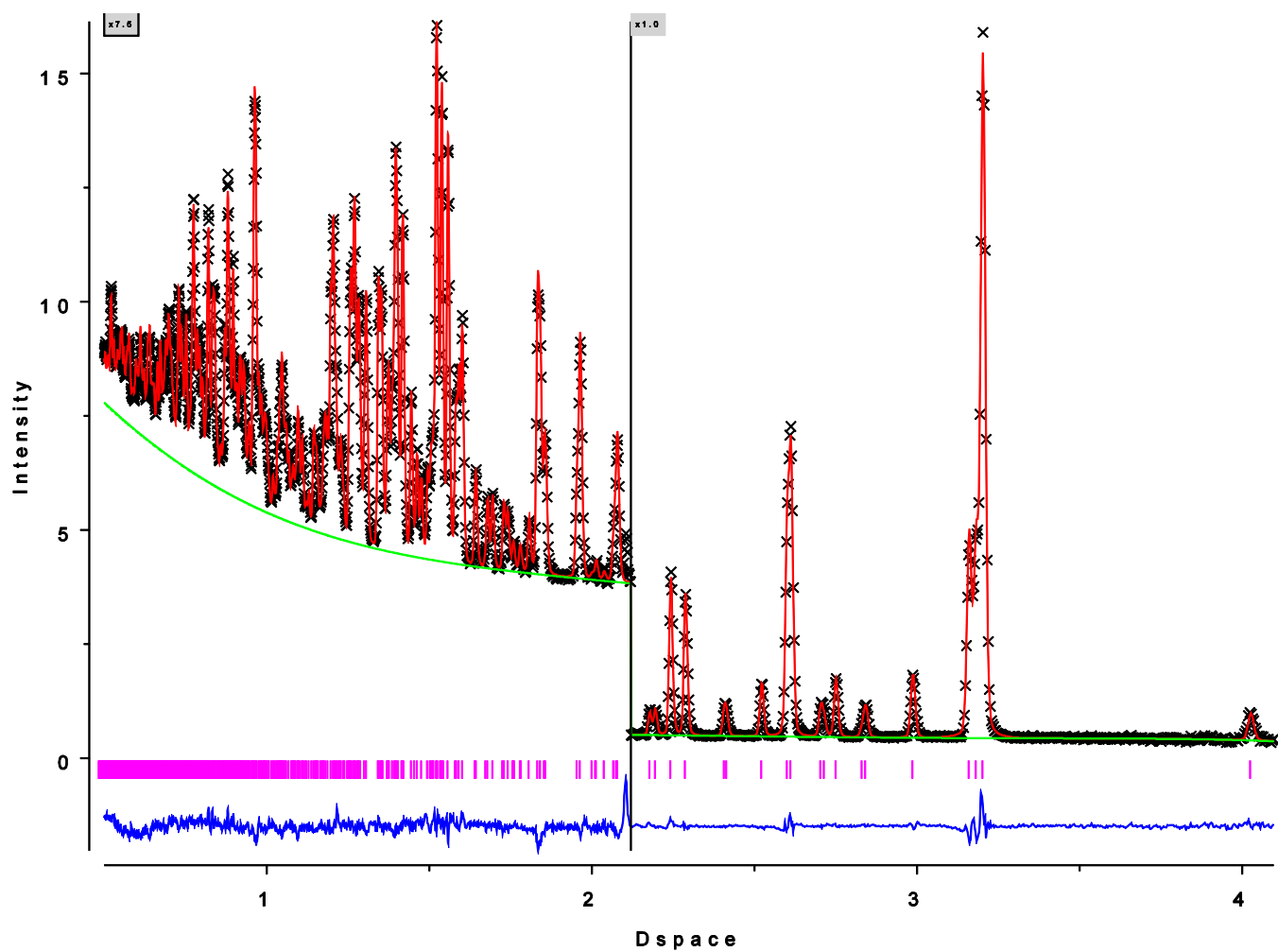


Figure2b Fitted neutron powder diffraction data from  $\text{ND}_4\text{IO}_3$  at 4.2K collected in the Polaris detector bank ( $\langle 2\theta \rangle = 92^\circ$ ) (magnified region x 7.5)



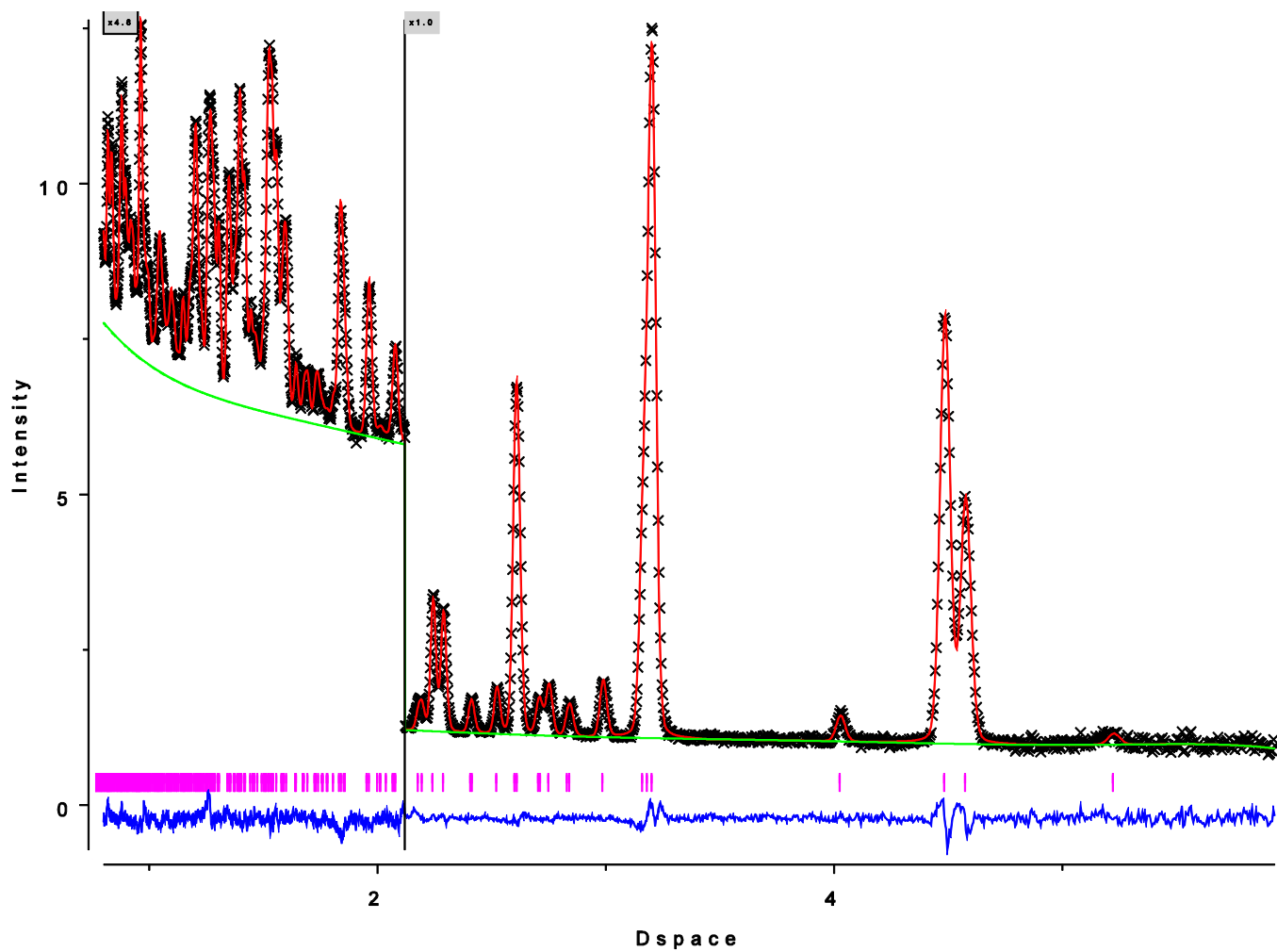


Figure2c Fitted neutron powder diffraction data from  $\text{ND}_4\text{IO}_3$  at 4.2K collected in the Polaris detector bank ( $\langle 2\theta \rangle = 52^\circ$ ) (magnified region x 4.8)

X = observed intensity, solid red calculated intensity, solid green background, solid blue difference, vertical pink lines reflection markers.

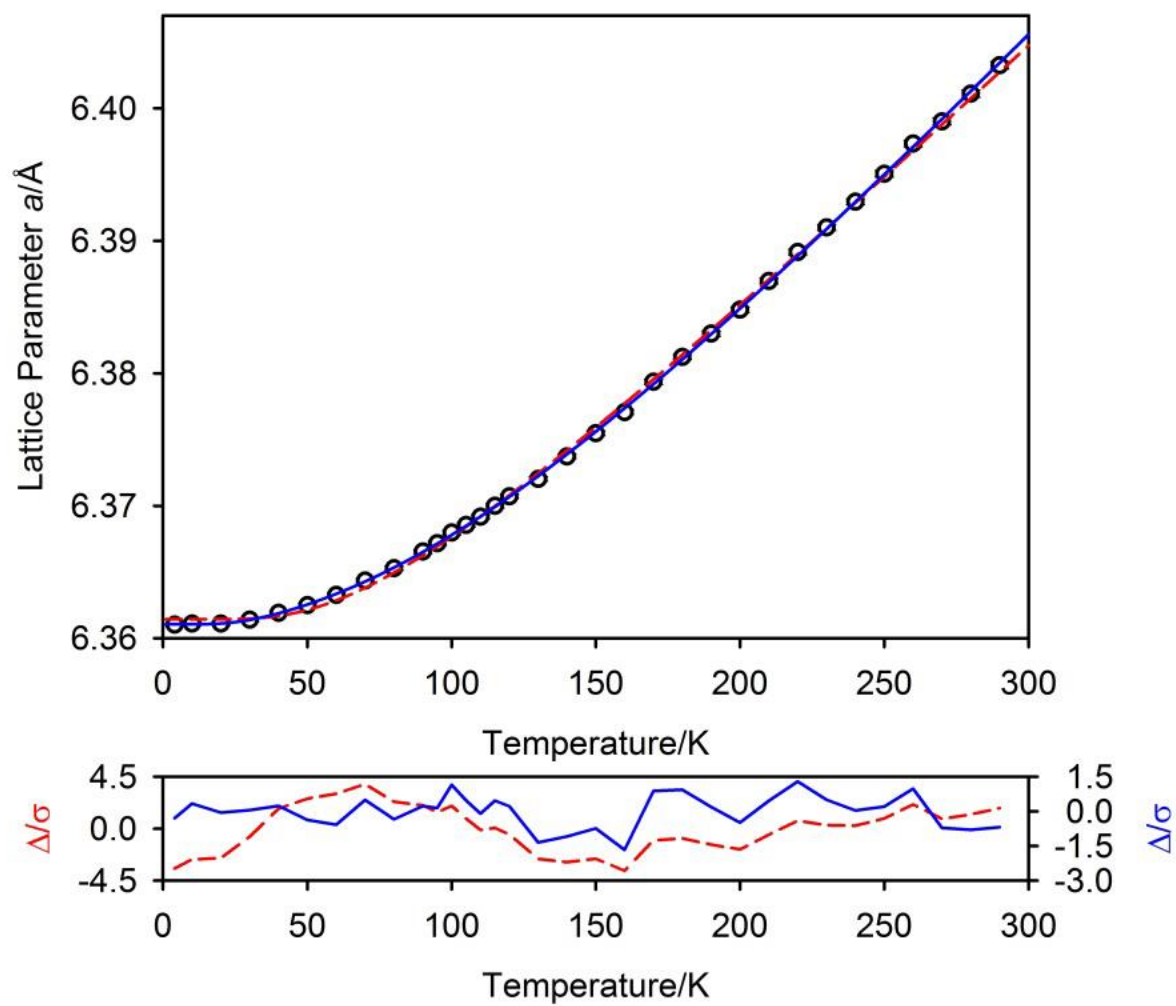


Figure 3a Variation in  $a$  with temperature, error bars are smaller than the symbols

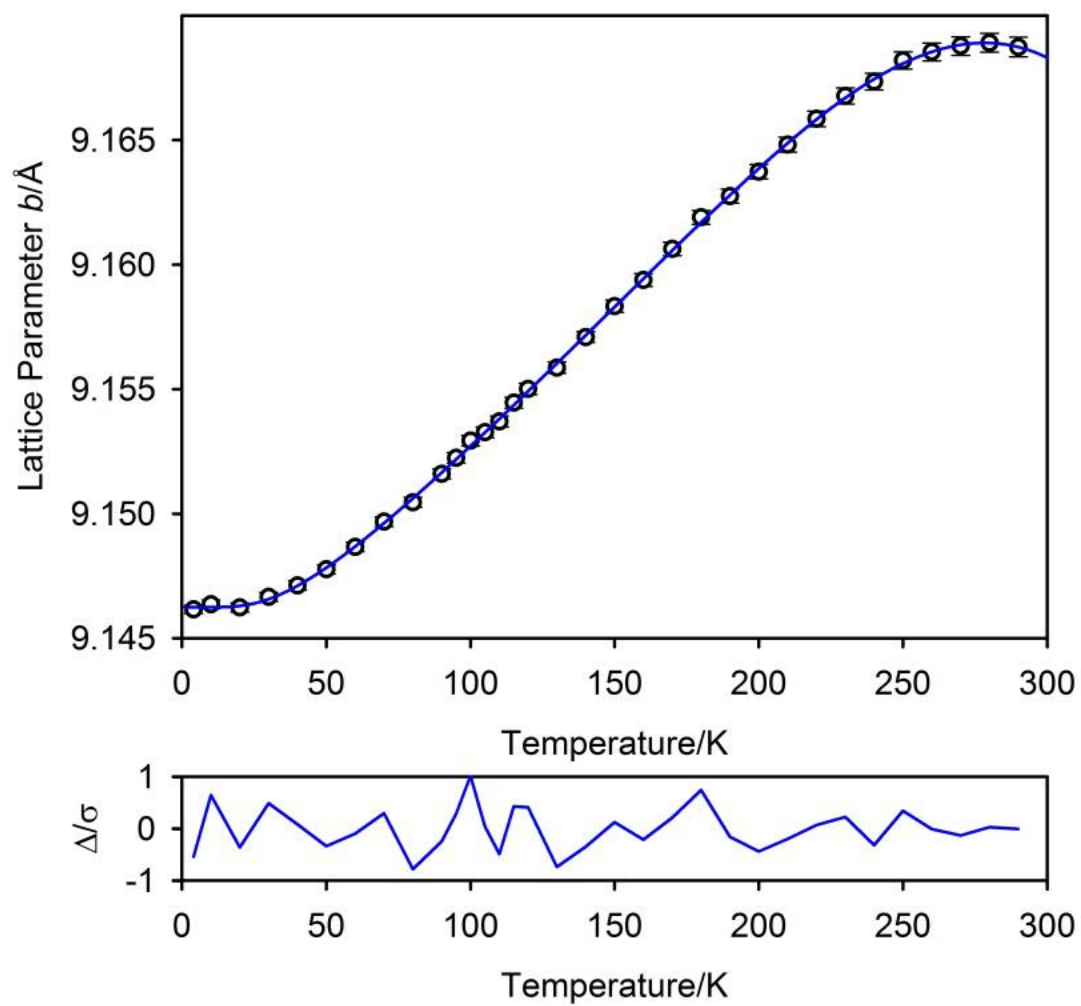


Figure 3b Variation in  $b$  with temperature

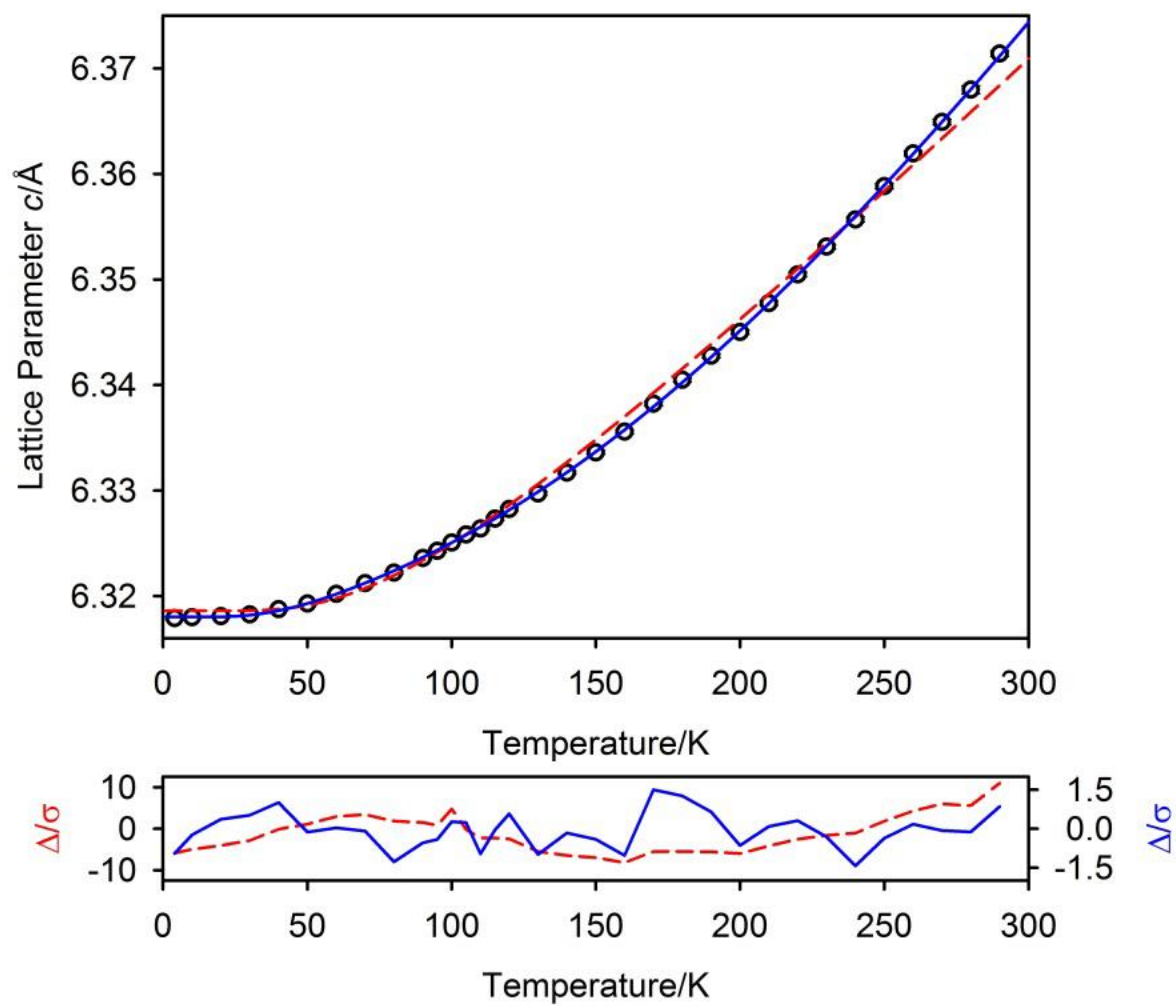


Figure 3c Variation in  $c$  with temperature

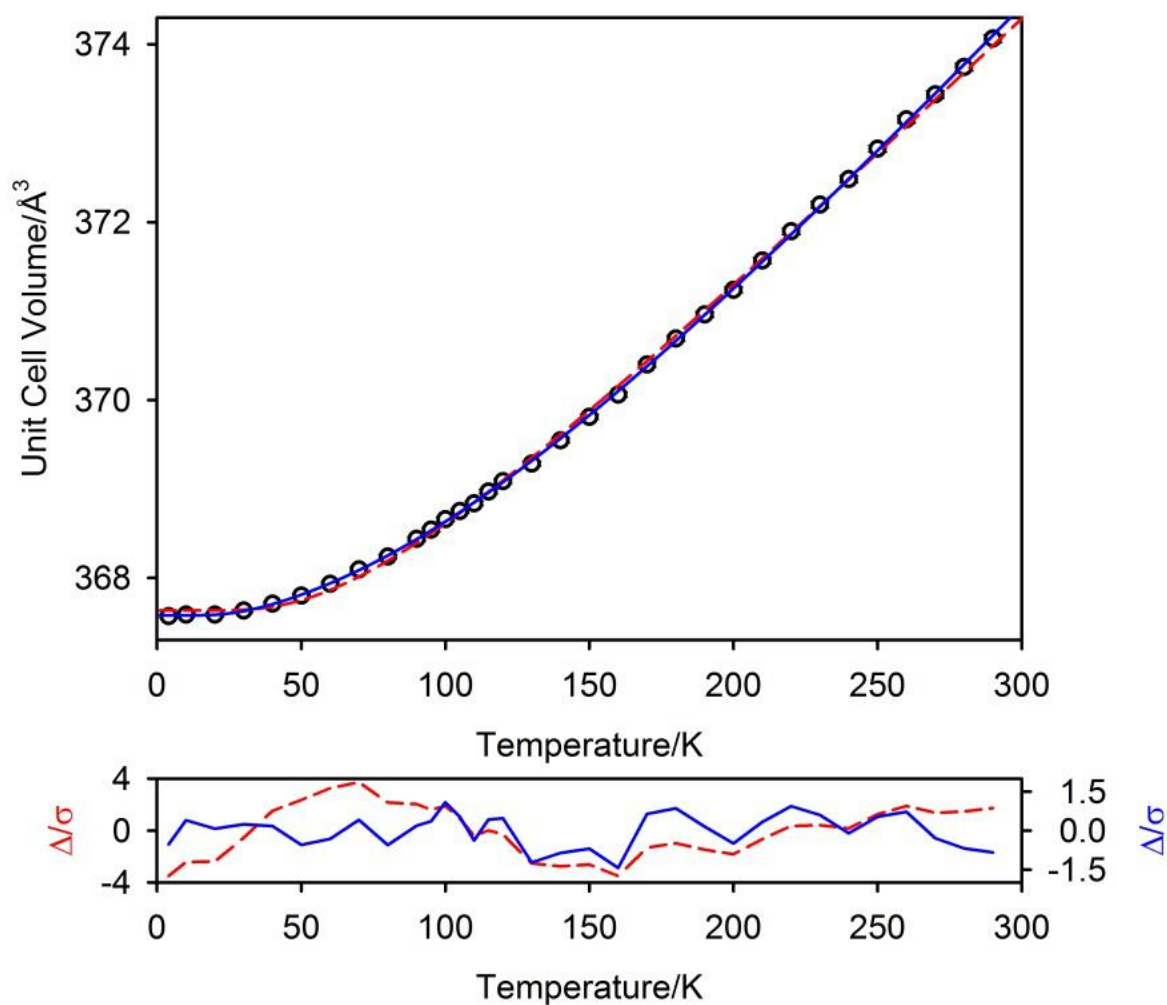


Figure 3d Variation in unit cell volume (V) with temperature

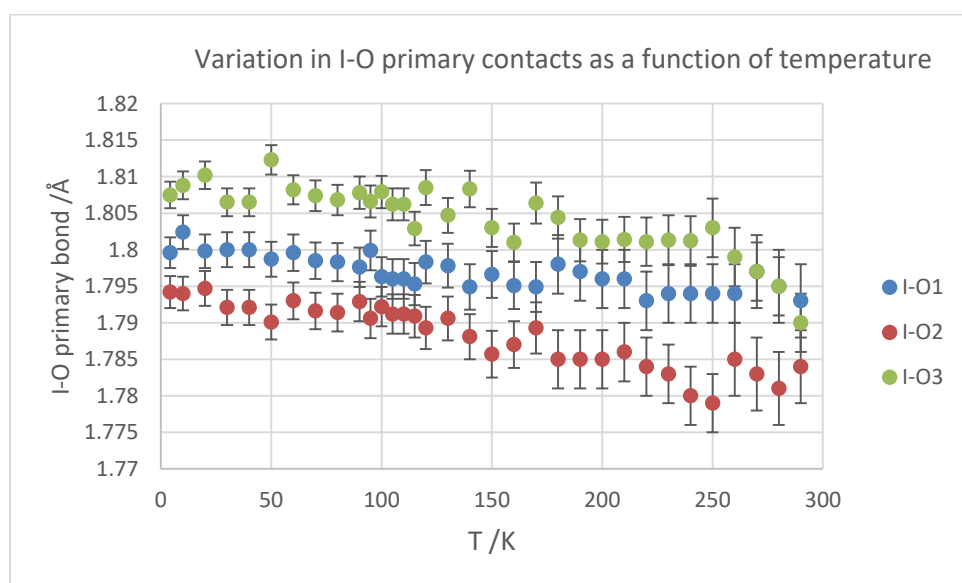


Figure 4a Variation in the primary bond lengths in the  $\text{IO}_3^-$  ion as a function of temperature

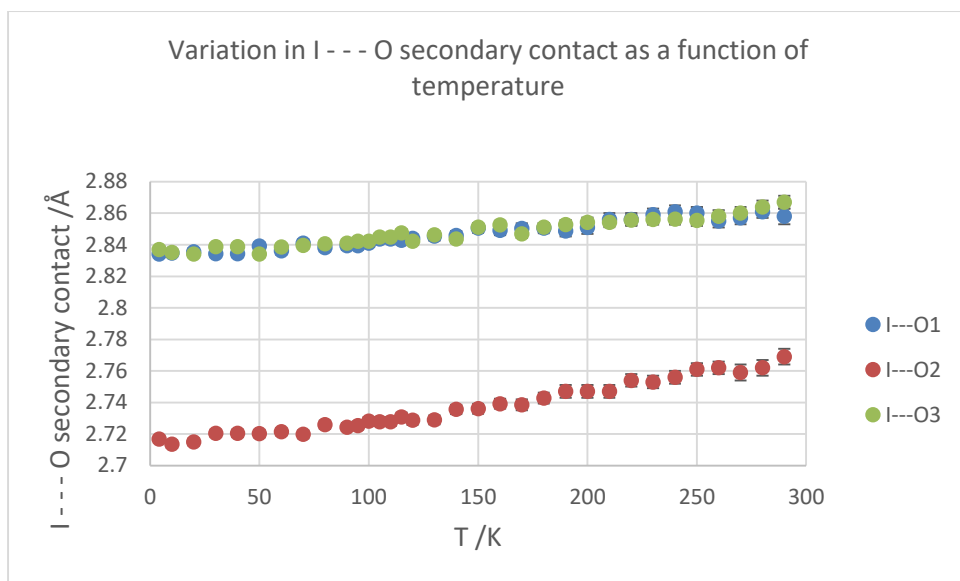


Figure 4b Variation in the I --- O secondary contacts as a function of temperature

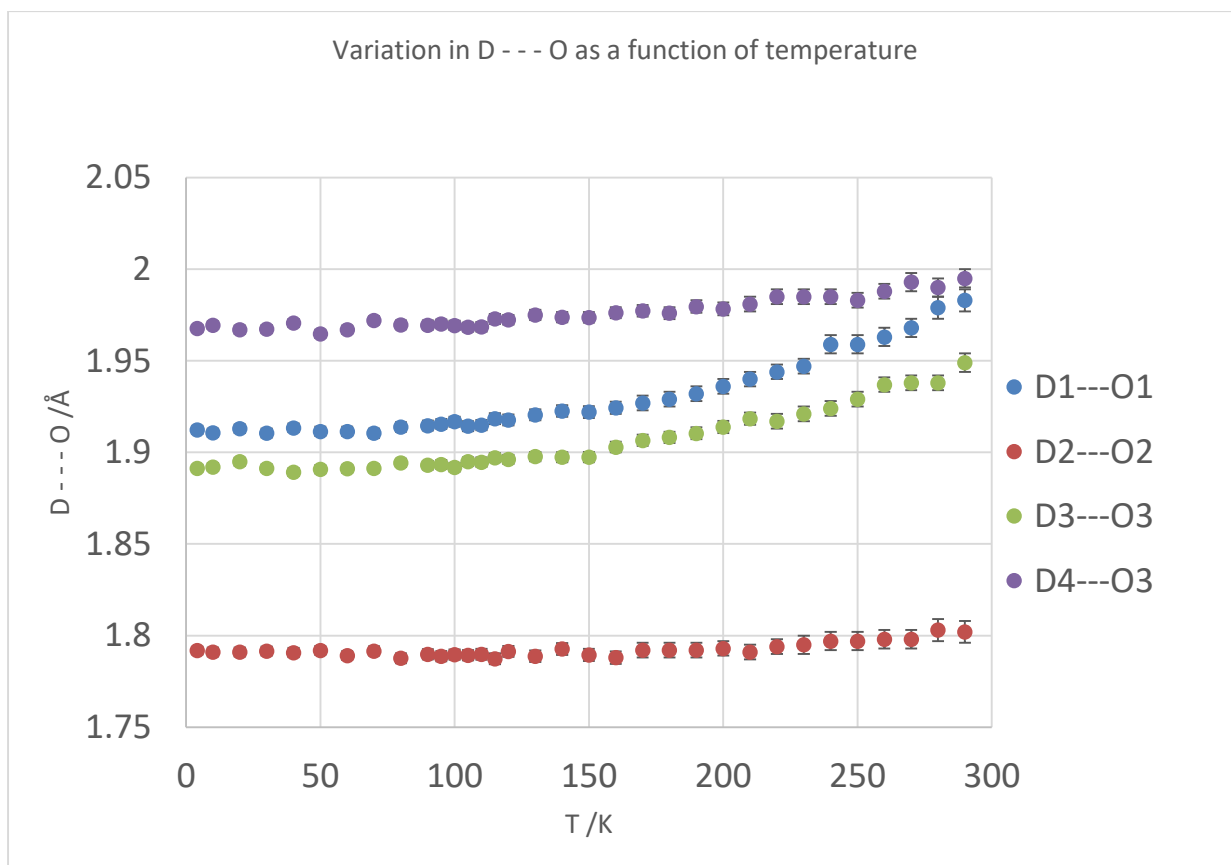


Figure 4c Variation in D --- O as a function of temperature

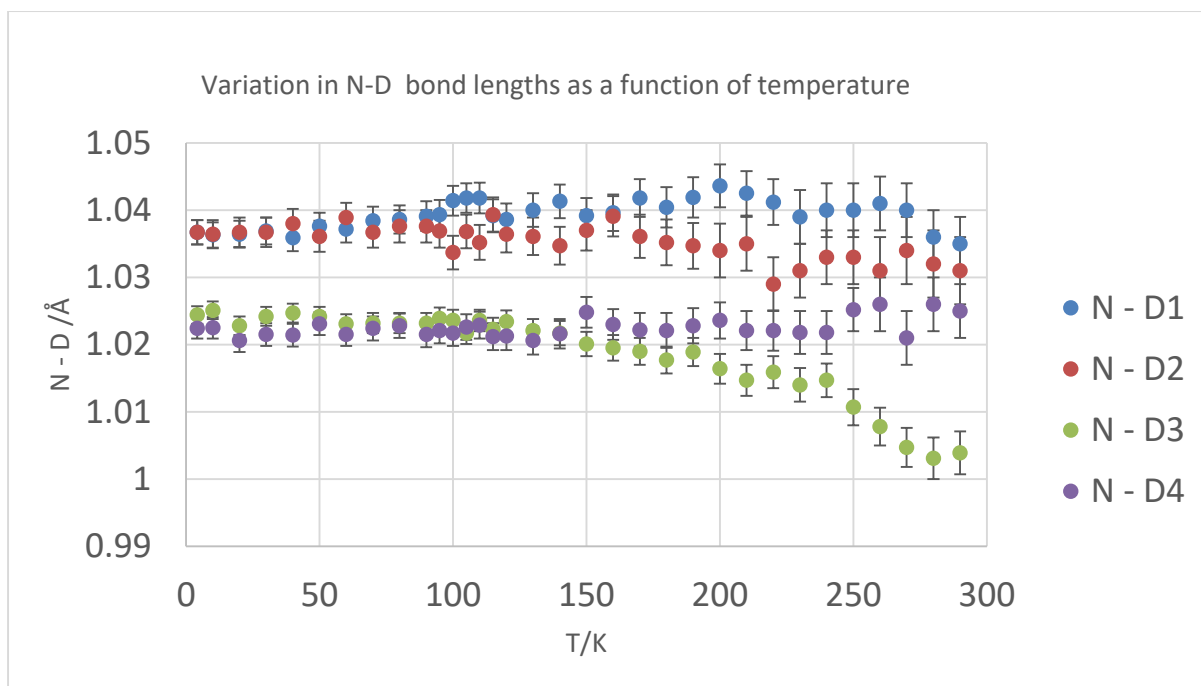


Figure 4d Variation of N-D bonds lengths as a function of temperature.

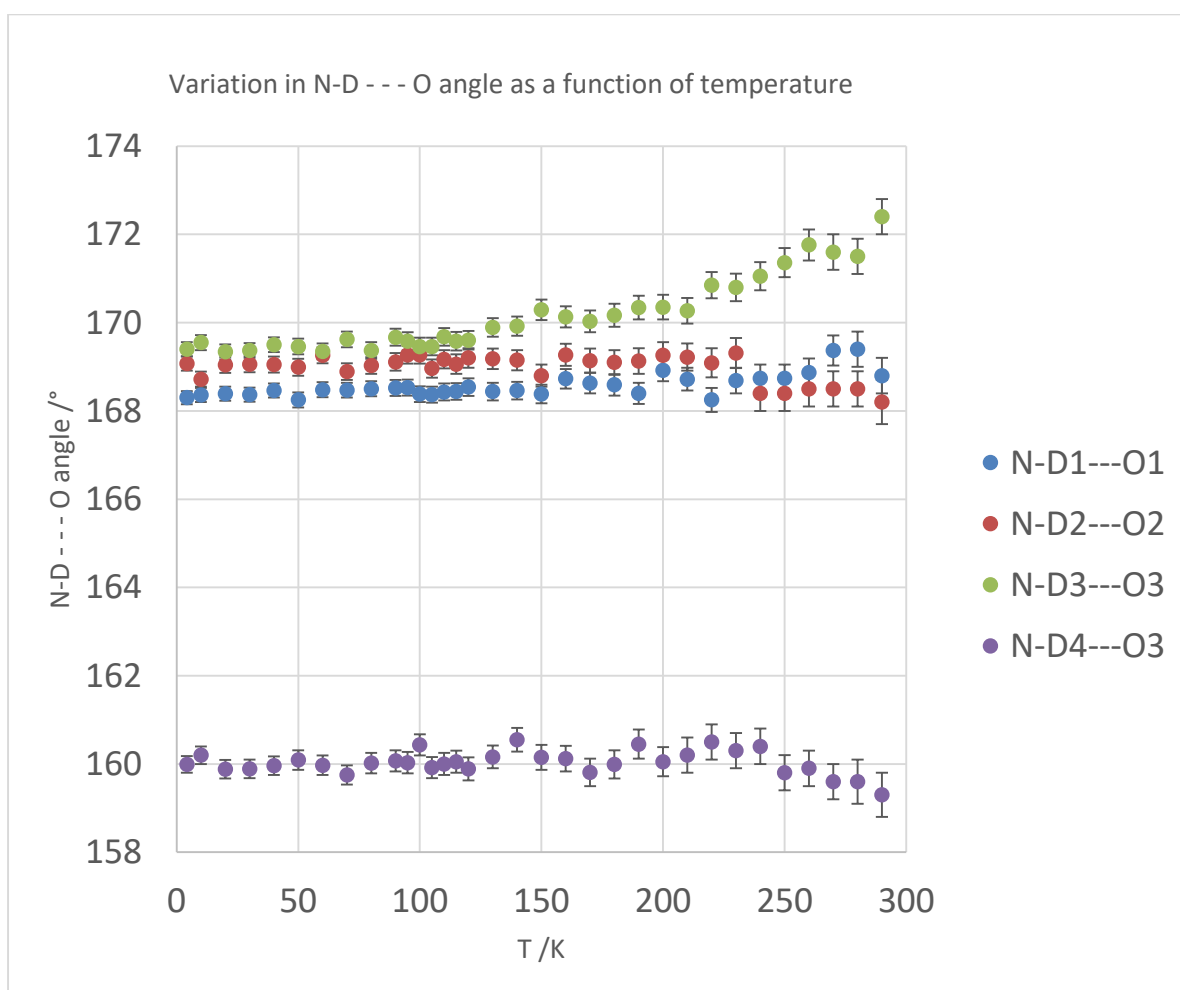


Figure 4e Variation in N-D - - - O angle as a function of temperature

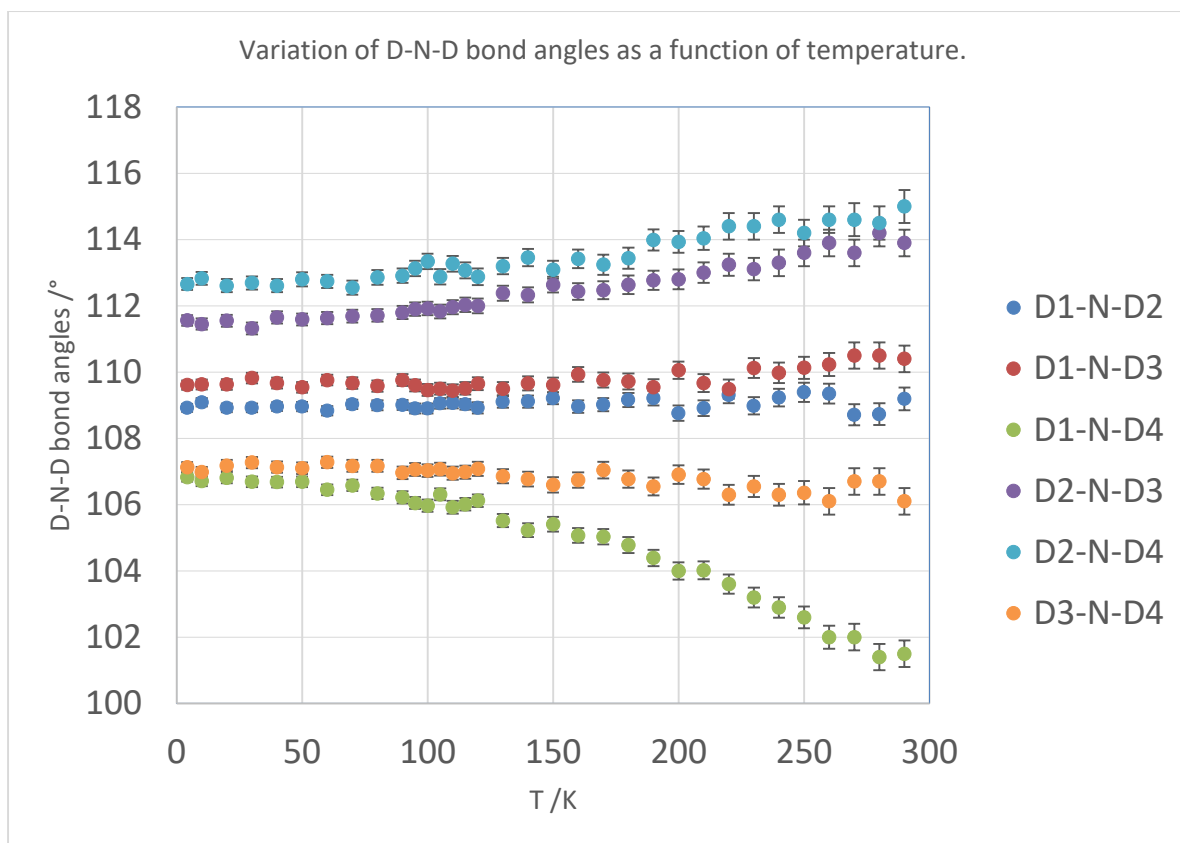


Figure 4f Variation of D-N-D bond angles as a function of temperature.

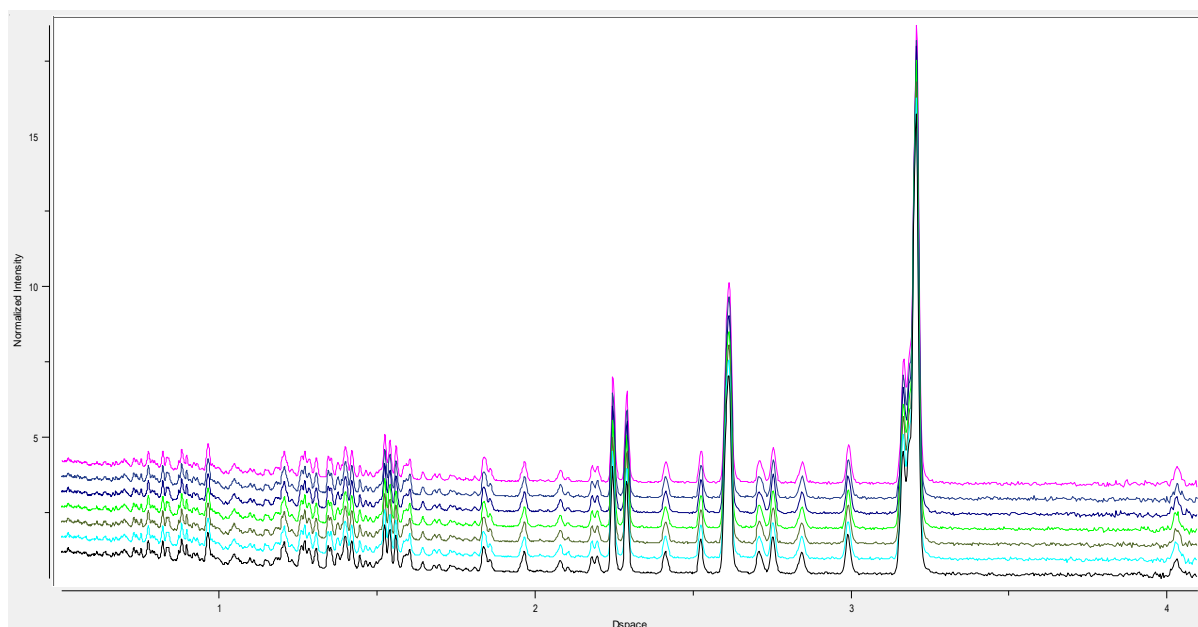


Figure 5 Stack plot Neutron powder diffraction patterns in the temperature range 90-120K Lowest plot 90K



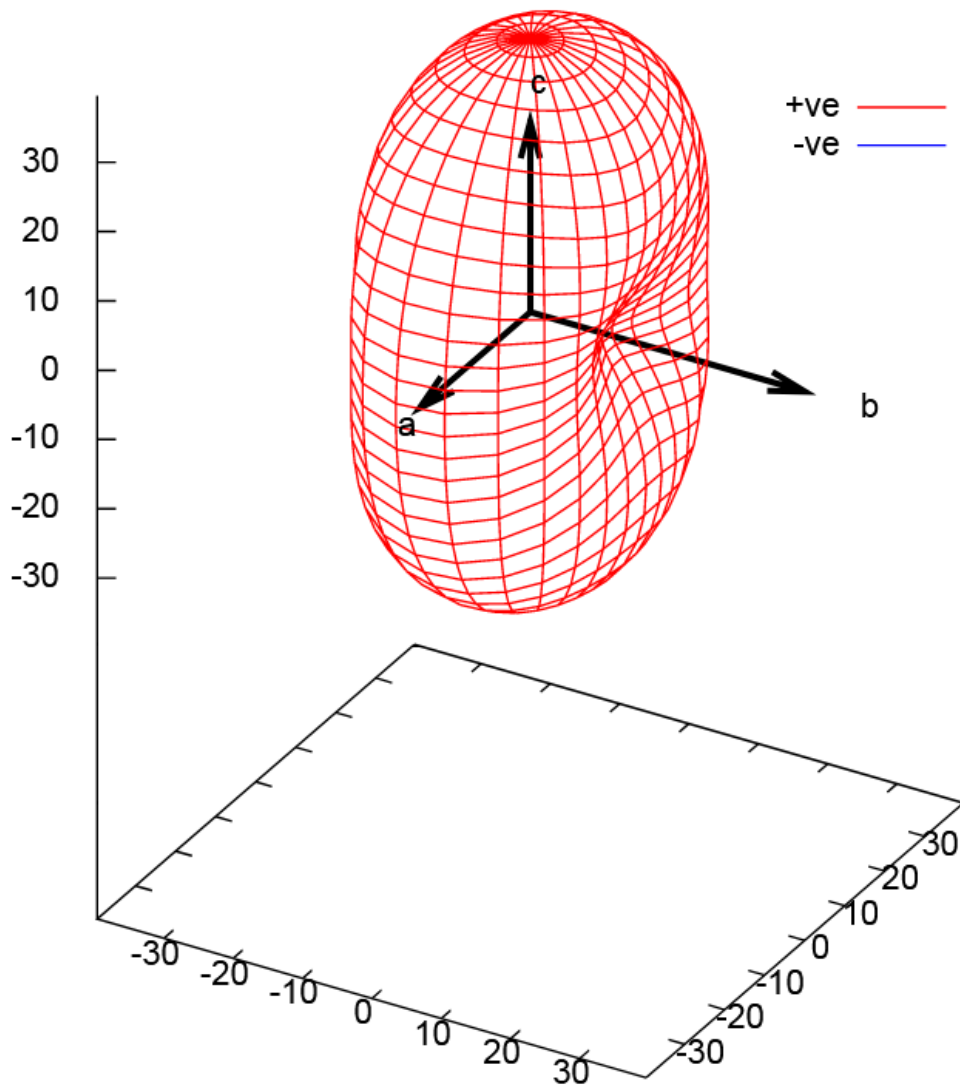


Figure 6 Expansivity indicatrix for linear portion of expansion. (150 – 250K)

Examination of the changes in the lattice parameters shows a smooth increase in the a- and c-axes as the sample is heated, with the rate of change increasing as the temperature rises. By contrast for the b-axis the graph shows a distinct sigmoidal shape, with expansion appearing to stop at about 270K; with the material possibly even contracting at temperatures above this.

The data in figure 3 shows fits to  $a(T) = a_0 + k/(\exp(E/T)-1)$ ,  $a_0$ : lattice parameter at 0 K, E: Einstein temperature, k: fitting constant that subsumes the effective bulk modulus and the effective Gruneisen constant.(dashed red line).The effect of modifying this model, by adding an additional term (ie  $a(T) = a_0 + k_1/(\exp(E_1/T)-1) + k_2/(\exp(E_2/T)-1)$ ), is shown as the blue full lines The fits assume that the lattice parameters behave in the same way, and for simplicity, the internal energy function is that of an Einstein oscillator (delta function in the phonon density of states). The b axis (as commented

on previously) is quite clearly different and a single Einstein expression would not fit these data (hence no red line fit). The two-term model, however, fits acceptably well but has  $k_2 < 0$  (ie a negative Gruneisen constant) which is clearly necessary to take account of the negative linear thermal expansion. For this to occur at the temperature it does, means that  $E_2$  is very large with respect to  $E_1$ . From these fits to the lattice parameters we conclude that these show no obvious premonitory behaviour for the low temperature transition. Further confirmatory evidence for the absence of a gross structural change can be seen in that there are no obvious changes in the diffraction pattern in the range 90-120K (figure 4)

## Discussion

For the linear portions of the graphs (100-250K) of the graph calculation of the expansion coefficients gives values of  $\alpha_a \alpha_b \alpha_c$  (30.8(2) 10.9(3) 39.6(6)  $\text{MK}^{-1}$ ). A contraction of the b axis (negative thermal expansion) has been previously reported in the temperature region which precedes the 368K phase transition (Viswanathan, & Salje 1975). Such a contraction at a ferroelectric transition is not unexpected and has been previously seen<sup>34</sup> for example in  $\text{PbTiO}_3$  and related materials with the perovskite structure (Rossetti *et al*; 1998; Glazer & Mabud 1978; Agrawal *et al* 1987; Agrawal *et al* 1988), and has been previously commented on in reviews on negative thermal expansion (Evans 1999), and is associated with the coordination around the six fold coordinated metal ion becoming more regular. This does not appear to be the case in  $\text{ND}_4\text{IO}_3$  where instead the differences between the primary and secondary contacts in the  $\text{IO}_3^-$  ion are increasing with temperature, although both the primary and secondary bond lengths become slightly more uniform. The lattice parameters that we determine are in good agreement with those obtained in two of the early studies (Keve, *et al*, 1971; Viswanathan K., & Salje, E. 1975). The small differences may be the result of deuteration which is a well-known effect in hydrogen bonded systems (Robertson and Ubbelohde 1939; Ubbelohde and Woodward 1945; Jeffrey 1998), but differ markedly from those obtained in a more recent study (Kader, *et al*, 2013), where the lattice parameters reported at 300K were  $a = 6.421(17)$ ,  $8.8752(79)$   $6.2510(59)$  compared to our results at 295K.

With regard to the interatomic contacts in this compound we will first examine the 3 hydrogen bonds that are weakest at ambient temperature. As the temperature is raised two of these interactions (N-D1---O1 and N-D3---O3) show a marked increase in the D---O distances above 110K with one of these D3---O3 being accompanied by increasing linearity of the N-D3---O3 angle. (See comment on lattice parameters mentioned above) A similar but less pronounced trend is also observed for the weakest hydrogen bond (N-D4---O3). Finally, it can be seen that the strongest hydrogen bond which consists of N-D2 and O2 shows only small changes in the N---O, D---O distances and the N-D---O angle with

temperature, implying that the strength of this hydrogen bond does not appreciably change with temperature. Thus it seems likely that the changes previously reported to occur at 103K are the result of the locking in of the hydrogen bonds below this temperature. These changes in the hydrogen bonding are also seen in the changes in the N-D bond lengths as a function of temperature. Here it can be clearly seen that N-D3 becomes significantly shorter in length as the hydrogen bond in which this atom is involved decreases in strength with increasing temperature. We believe that this is a genuine effect rather than effects associated with libration because the deuterium atoms whose changes in hydrogen bonding are not as dramatic, figures 4d ,4e, 4f) do not appear to show this effect.

The changes caused by temperature on the O-I---O moieties is far less pronounced. Whilst there is an increase in the primary I-O bond lengths on raising the temperature (figure 4a) it is much smaller than the changes observed in the secondary I---O interactions. There is a small increase in the I---O distances (figure 4b) from about 77.5% to 78.4% of the van der Waals radii. This by itself does not preclude a charge transfer model as the changes in the bond order in such a system are not linear (Burgi 1975; Dunitz 1995). However, a more likely cause of the shortening of the primary covalent bonds at higher temperatures is due to the librational motion of the  $\text{IO}_3^-$  ions at higher temperatures. Unfortunately, because we were unable to obtain reliable anisotropic atomic displacement parameters from the powder diffraction data (unsurprisingly) and thus we were unable to test this hypothesis which in practice could be determined by a full single crystal analysis.

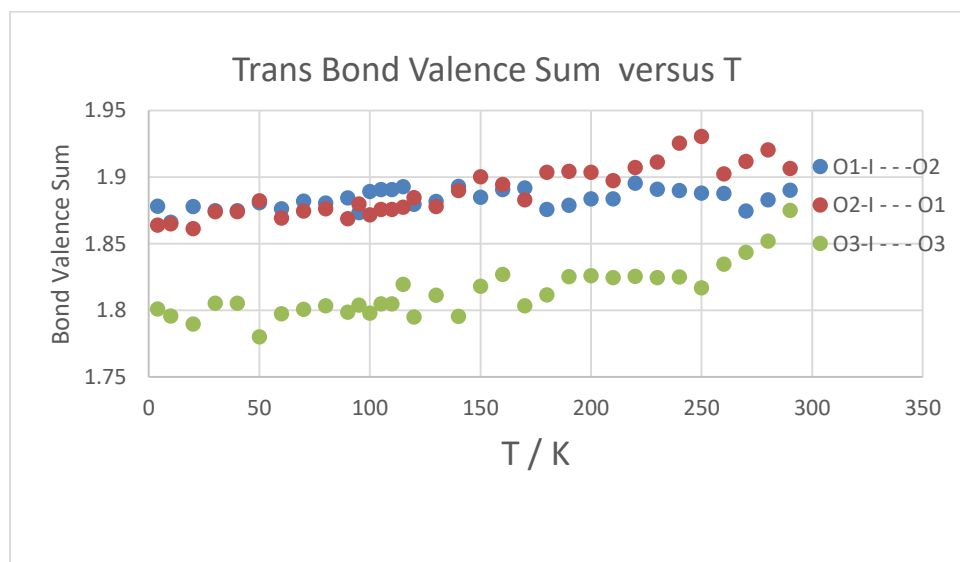


Figure 7 Bond Valence Sums for trans O-I - - - O moieties versus temperature

We have performed a bond valence calculation on the system (Brown & Altermatt 1985), whilst the sums at the oxygen atoms (when taking account of additional hydrogen bonding) are plausible, the valence sum at iodine is approximately + 5.5 significantly higher than the formal oxidation state of

+5. Figure 7 shows the bond valence sums for the trans O-I - - - O units. The deficiency in the bond valence sum of 2 at oxygen is made up by the contribution of the hydrogen bonds. It can be seen that for all the units there is in general an increase in the bond valence sum with increasing temperature, and what is striking about the graph is that for O3-I - - -O3 there is a marked increase in the valence sum as the temperature is raised, starting at about 250 K. Looking at figure 1e we see that this unit is aligned almost parallel to b. We previously noted that the thermal expansion of b starts to decrease rapidly at this temperature and is known in the hydrogenous form to produce negative thermal expansion as the temperature is increased further (Viswanathan, & Salje, 1975). Thus the decrease in hydrogen bonding (note O3 is acting as an acceptor to 2 hydrogen bonds) with increasing temperature leads to incipient regularization of the  $\text{IO}_3^-$  pyramids with concomitant negative thermal expansion in the direction of regularization. This can also be seen by the marked decrease in the I-O3 primary bond length above approximately, 250K (figure 4a). Further evidence that it is the loss of hydrogen bonding and not regularization of the pyramidal  $\text{IO}_3^-$  ions in themselves that is responsible for this phenomenon is given by it appearing to start at a lower temperature in the deuterated form that we studied compared to the protonated form (Viswanathan, & Salje, 1975) , where contraction is known to start no lower in temperature than 293K. This is because hydrogen bonding involving deuterium was shown to be weaker than that involving hydrogen, in imidazole at around 353K (Grimson 1963), and more recently it has been shown (Scheiner, & Čuma 1996) that hydrogen bonds irrespective of their nature (predominantly covalent or ionic) involving deuterium are weaker than those involving hydrogen at higher temperatures. Thus we would expect the loss of hydrogen bonding to occur at a lower temperature for the deuterated compound. Thus from our limited data it appears that the hydrogen bonds are involved in inhibiting regularization of the  $\text{IO}_3^-$ . A further effect of hydrogen bonding is also seen if we look at the thermal expansion in the ac plane. Here it can be seen that the two hydrogen bonds involving O3 lie mainly in this plane (figure 1e). Since the change in hydrogen bonding with temperature is more pronounced for the hydrogen bonds in this plane and that involving D3 is more pronounced than that for D4 we would expect the expansion to be larger for that involving D3 which is aligned with c, followed by that involving D4, which is aligned  $\sim 15^\circ$  away from a direction, and this is reflected in the magnitudes of  $\alpha_a$   $\alpha_b$   $\alpha_c$  (30.8(2), 10.9(2) 39.6(6)  $\text{MK}^{-1}$ ).

As we commented on in the introduction two previous studies on the dielectric properties of these materials have been carried out (Salje 1974; Kaderet *al* 2013 ). The earlier study does not permit detailed interpretation as neither dielectric loss data nor the frequency used to determine the permittivity are given, consequently all that can be deduced is that there appears to be a peak in the permittivity at 100K. More recent studies show a much smaller frequency dependent value for  $\epsilon'$ . Frequency dependency was also observed for  $\epsilon''$ , with  $\epsilon''$  increasing as the frequency is increased,

indicating that there may be a degree of relaxation but only at very high frequencies. In addition, the D-E loops do not show any saturation. Taking these results together indicates that the material at low temperature does not display ferroelectricity but rather is a "lossy" dielectric which may be associated with the reduced motion of the ammonium ions at low temperature. Further evidence for this can be seen a proton spin relaxation NMR study in this material (Shenoy & Ramakrishna 1983) between 100 and 425K, who concluded that their results were "typical of a hindered solid with motions freezing around 77 K". Our results suggest that this freezing occurs rather at 100 K and is responsible for the observed changes in dielectric behaviour.

## Conclusion

In conclusion we have established the following points

Firstly the changes in the dielectric properties of the material at 103K are not the results of a structural phase transition involving changes in either symmetry or large changes in the size of the unit cell but rather a maximization of the hydrogen bonding on cooling of the three hydrogen bonds that are weakest at room temperature. Secondly the uniaxial contraction of the b axis prior to the phase transition at 355K starts to occur at temperatures below 273K in the deuterated form and is caused by the reduction in the extent of hydrogen bonding to the oxygen atoms involved in the O-I---O unit which is oriented approximately parallel to this axis. This lower temperature compared to the protonated form is the result of the lower strength of hydrogen bonds involving deuterons compared to protons. Finally, both the magnitude and changes in the magnitude of the thermal expansion coefficients are primarily driven by the changes in hydrogen bonding.

## Acknowledgments

We thank the STFC for provision of neutron beam time. We would like to acknowledge helpful advice and comments from Professor Derek Sinclair. We wish to recognize the contribution of the late William George (Bill) Marshall to this project from the conception, execution, and analysis of the data and his contribution to the use of neutron diffraction to the study of hydrogen bonding in condensed matter.

## References

- Abdel-Kader, M. M., El-Kabbany, F., Naguib, H. & Gamal, W. M. (2008). *Phase Transitions*. **81**, 83-99.
- Agrawal, D. K., Halliyal, A. & Belsick, J. (1988). *Mater. Res. Bull.* **23**, 159-164.
- Agrawal, D. K., Roy, R. & Mckinstry, H. A. (1987). *Mater. Res. Bull.* **22**, 83-88.
- Alcock, N. W. (1972). *Adv Inorg. Chem. Radiochem.* **15**, 1-58.
- Auffinger, P., Hays, F. A., Westhof, E. & Ho, P. S. (2004). *Proc. Natl. Acad. Sci. U. S. A.* **101**, 16789-16794.
- Barabash, A. I. (1999). *J. Mol. Struct.* **508**, 81-85.
- Barabash, A., Gavrilko, T., Eshimov, K., Puchkovskaya, G. & Shanchuk, A. (1999). *J. Mol. Struct.* **511**, 145-152.
- Bergman, J. G., Boyd, G. D., Ashkin, A., & Kurtz, S. R. (1969). *Journal of Applied Physics* **40**, 2860-2863.
- Bertani, R., Sgarbossa, P., Venzo, A., Lelj, F., Amati, M., Resnati, G., Pilati, T., Metrangolo, P. & Terraneo, G. (2010). *Coord. Chem. Rev.* **254**, 677-695.
- Bismayer, U., Salje, E. & Viswanathan, K. (1979). *Zeitschrift Fur Kristallographie*. **149**, 179.
- Brinck, T., Murray, J. S. & Politzer, P. (1992). *International Journal of Quantum Chemistry*. 57-64.
- Brown, I. D. & Altermatt, D. (1985). *Acta Crystallographica Section B-Structural Science*. **41**, 244-247.
- Burgi, H. B. (1975). *Angewandte Chemie-International Edition in English*. **14**, 460-473.
- Cai, W. & Katrusiak, A. (2013). *Dalton Transactions*. **42**, 863-866.
- Cavallo, G., Metrangolo, P., Milani, R., Pilati, T., Priimagi, A., Resnati, G. & Terraneo, G. (2016). *Chem. Rev.* **116**, 2478-2601.
- Cho, C. M., Wang, X., Li, J. J., He, C. & Xu, J. (2013). *Liquid Crystals*. **40**, 185-196.
- Clark, T., Hennemann, M., Murray, J. S. & Politzer, P. (2007). *Journal of Molecular Modeling*. **13**, 291-296.
- Cliffe, M. J. & Goodwin, A. L. (2012). *J. Appl. Crystallogr.* **45**, 1321-1329.
- Dunitz, J. D. X-ray Analysis & the structure of Organic Molecules 2<sup>nd</sup> edition VCH Basel (1995).
- Endo, S., Chino, T., Tsuboi, S. & Koto, K. (1989). *Nature*. **340**, 452-455.
- Evans, J. S. O. (1999). *J. Chem. Soc. -Dalton Trans.* 3317-3326.

- Fukami, T., Akahoshi, S., Hukuda, K. & Yagi, T. (1987). *Journal of the Physical Society of Japan*. **56**, 4388-4392.
- Glazer, A. M. & Mabud, S. A. (1978). *Acta Crystallographica Section B-Structural Science*. **34**, 1065-1070.
- Grabowski, S. J. (2013). *Physical Chemistry Chemical Physics*. **15**, 7249-7259
- Grimison, A. (1963) *J. Phys. Chem.*, 1963, **67**, 962–964.
- Jeffrey, G. A. An Introduction to Hydrogen Bonding Oxford University Press: New York and Oxford. (1997).
- Jones, R. H., Knight, K. S., Marshall, W. G., Clews, J., Darton, R. J., Pyatt, D., Coles, S. J., & Horton, P. N., *Crystengcomm* (2014). **16**, 237 -243.
- Jones, R. H., Knight, K. S., Marshall, W. G., Coles, S. J., Horton, P. N. & Pitak, M. B., *Crystengcomm* (2013). **15**, 8572. -8677.
- Keve, E. T., Abrahams, S. C., & Bernstein, J.L. (1971). *J. Chem. Phys.* **54**, 2566
- Kader, M. M. A., El-Kabbany, F., Naguib, H. M. & Gamal, W. M. (2013). *Phase Transitions*. **86**, 947-958.
- Kobayashi, Y., Endo, S., Koto, K., Kikegawa, T. & Shimomura, O. (1995). *Physical Review B*. **51**, 9302-9305.
- Larson, A. C., & Von Dreele, R. B. "General Structure Analysis System (GSAS)", Los Alamos National Laboratory Report LAUR 86-748 (2000);
- Lasave, J., Koval, S., Dalal, N. S. & Migoni, R. L. (2007). *Phys. Rev. Lett.* **98**, 267601.
- Lu, Y., Wang, Y., Xu, Z., Yan, X., Luo, X., Jiang, H. & Zhu, W. (2009). *J Phys Chem B*. **113**, 12615-12621.
- Marshall, W. G., Jones, R. H. & Knight, K. S. (2018). *Crystengcomm*. **20**, 3246-3250.
- Marshall, W. G., Jones, R. H., Knight, K. S., Clews, J., Darton, R. J., Miller, W., Coles, S. J. & Pitak, M. B. (2017). *Crystengcomm*. **19**, 5194-5201.
- McAllister, L. J., Praesang, C., Wong, J. P. -, Thatcher, R. J., Whitwood, A. C., Donnio, B., O'Brien, P., Karadakov, P. B. & Bruce, D. W. (2013). *Chemical Communications*. **49**, 3946-3948.
- Metrangolo, P., Neukirch, H., Pilati, T. & Resnati, G. (2005). *Acc. Chem. Res.* **38**, 386-395.
- Nguyen, H. L., Horton, P. N., Hursthouse, M. B., Legon, A. C. & Bruce, D. W. (2004). *J. Am. Chem. Soc.* **126**, 16-17.
- Oka, T., Mitsui, T., Shiroishi, Y. & Sawada, S. (1976a). *Journal of the Physical Society of Japan*. **40**, 913-914.

Oka, T., Mitsui, T., Shiroishi, Y. & Sawada, S. (1976b). *Journal of the Physical Society of Japan*. **40**, 913-914.

Olejniczak, A., Aniola, M., Szafranski, M., Budzianowski, A. & Katrusiak, A. (2013). *Crystal Growth & Design*. **13**, 2872-2879.

Peres, N., Souhassou, M., Wyncke, B., Gavaille, G., Cousson, A. & Paulus, W. (1997). *Journal of Physics-Condensed Matter*. **9**, 6555-6562.

Politzer, P. & Murray, J. S. (2013). *Chemphyschem*. **14**, 278-294.

Politzer, P. & Murray, J. S. (2012). *Theoretical Chemistry Accounts*. **131**, 1114.

Politzer, P., Riley, K. E., Bulat, F. A. & Murray, J. S. (2012a). *Computational and Theoretical Chemistry*. **998**, 2-8.

Praesang, C., Nguyen, H. L., Horton, P. N., Whitwood, A. C. & Bruce, D. W. (2008). *Chemical Communications*. 6164-6166.

Richards, R. E. & Schaefer, T. (1961). *Transactions of the Faraday Society*. **57**, 210,

Rietveld, H M. (1969) *J. Appl. Cryst.* **2**, 65-71.

Rissanen, K. (2008). *Crystengcomm*. **10**, 1107-1113.

Robertson, J. M. & Ubbelohde, A. R. (1939). *Proc. Roy Soc* **170**, 222-240,

Rossetti, G. A., Cline, J. P. & Navrotsky, A. (1998). *J. Mater. Res*. **13**, 3197-3206.

Rowland, R. S. & Taylor, R. (1996). *J. Phys. Chem*. **100**, 7384-7391.

Salje, E. (1974). *Acta Crystallographica Section a*. **A 30**, 518-521.

Salje, E. & Bismayer, U. (1977a). *Opt. Commun*. **20**, 303-304.

Scheiner, S. & Cuma, M. (1996). *J. Am. Chem. Soc*. **118**, 1511-1521.

Scholfield, M. R., Vander Zanden, C. M., Carter, M. & Ho, P. S. (2013). *Protein Science*. **22**, 139-152.

Shenoy, R. K. & Ramakrishna J. (1983). *Ferroelectrics*. **48**, 309-312.

Tibballs, J. E., Nemes, R. J. & McIntyre, G. J. (1982). *Journal of Physics C-Solid State Physics*. **15**, 37-58.

Toby, B. H. (2001). *Journal of Applied Crystallography*. **34**, 210-213.

Ubbelohde, A. R. & Woodward, I. (1942). *Proc Roy. Soc.* **179**, 399-407.

Umebayashi, H., Frazer, B. C., Shirane, G., & Daniels, W. B. (1967). *Solid State Commun*. **5**, 591-594.



van Laar, B. & Schenk, H. (2018). *Acta Crystallographica A-Foundation and Advances*. **74**, 88-92.

Viswanathan, K. & Salje, E. (1975). *Acta Crystallographica Section a*. **31**, 810-813.

Zhang, T., Chen, L., Gou, M., Li, Y., Fu, D. & Xiong, R. (2010). *Crystal Growth & Design*. **10**, 1025-1027.